Low-temperature vibrational properties of KGd(WO): (Er, Yb) single crystals studied by Raman spectroscopy

D. Kasprowicz, T. Runka, A. Majchrowski, E. Michalski

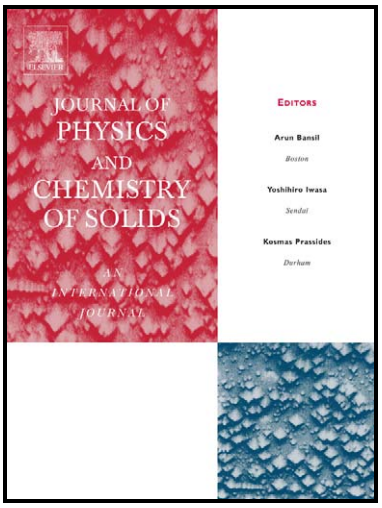

www.elsevier.com/locate/jpcs

Low-temperature vibrational properties of $KGd(WO_4)_2$: (Er, Yb) single crystals studied by Raman spectroscopy

D. Kasprowicz, T. Runka, A. Majchrowski, E. Michalski

PII: S0022-3697(09)00162-0
DOI: doi:10.1016/j.jpcs.2009.07.015
Reference: PCS 5889

To appear in: *Journal of Physics and Chemistry of Solids*

Received date: 12 March 2008
Revised date: 31 December 2008
Accepted date: 1 July 2009

Cite this article as: D. Kasprowicz, T. Runka, A. Majchrowski and E. Michalski, Low-temperature vibrational properties of $KGd(WO_4)_2$: (Er, Yb) single crystals studied by Raman spectroscopy, *Journal of Physics and Chemistry of Solids*, doi:10.1016/j.jpcs.2009.07.015

Low-temperature vibrational properties of $KGd(WO_4)_2$: (Er, Yb) single crystals studied by Raman spectroscopy

D. Kasprowicz[1*] , T. Runka[1], A. Majchrowski[2] and E. Michalski[2]

[1]*Faculty of Technical Physics, Poznan University of Technology, Nieszawska 13 A, 60 - 965 Poznań, Poland*

[2]*Institute of Applied Physics, Military University of Technology, Kaliskiego 2, 00 - 908 Warsaw, Poland*

Abstract – Temperature-dependent polarized Raman spectra of $KGd(WO_4)_2$: (Er, Yb) single crystals have been analyzed over the 77 – 292 K temperature range. The A_g and B_g spectra obtained are discussed in terms of factor group analysis. The spectra have been found to reveal the bands related to internal and external vibrations of WO_4^{2-} ,WOW and WOOW molecular groups. Strong depolarization of the majority of the Raman bands has been observed in the whole temperature range. Some anomalies in the spectral parameters of selected Raman bands below 175 K have been discussed in terms of the local distortion of WO_4^{2-} ions in $KGd(WO_4)_2$: (Er, Yb) crystals.

Keywords: **A.** Optical materials; **C.** Raman spectroscopy; **D.** Lattice dynamics

1. Introduction

* Corresponding author. Tel.: +48 61 665 3168; fax: +48 61 665 3164.
E-mail address: dobkas@phys.put.poznan.pl (D. Kasprowicz).

Potassium gadolinium tungstate crystals $KGd(WO_4)_2$ (KGW) doped with rare earth ions are very attractive solid state laser materials with interesting optical properties [1–5]. The up-conversion processes in these materials produce the highly efficient stimulated emission in the visible spectral range with infrared laser diode excitation. The Er^{3+} doped KGW crystals show the efficient green photoluminescence excited by diode lasers in the 795 – 805 nm and 970 – 990 nm spectral range. They can be also used in construction of the eye-safe diode-pumped lasers emitting at 1.5 μm. In order to improve the diode-pumping efficiency of the Er^{3+} doped KGW crystal, it is co-doped with Yb^{3+} ions. The Yb^{3+} ions are characterized by a strong and broad absorption band in the 900 – 1025 nm range that allows resonant energy transfer between Yb^{3+} and Er^{3+} ions. The excitation tuning in the 920 – 1000 nm wavelength region in KGW: Er^{3+} crystals co-doped with Yb^{3+} ions and the large overlap between ytterbium emission and erbium absorption produce the optimal up-conversion efficiency and laser emission [6,7]. The energy transfer between Yb^{3+} and Er^{3+} ions are phonon-assisted processes, influenced by the number of excitations related to the crystal field of the host material. The high energy stretching modes of the tungsten-oxygen vibrations in KGW crystals can be effective in these processes. The vibrational properties some tungstates doped with trivalent rare earth ions have been already investigated [8–13]. However, still little is known on their vibrational properties in the low–temperature region.

KGW crystals have the monoclinic structure with $C2/c \equiv C_{2h}^6$ space group (Z = 4) at room temperature. The lattice cell parameters are: a = 10.652 Å, b = 10.374 Å, c = 7.582 Å, β = 130.80° [14]. In KGW structure the tungsten and oxygen atoms form octahedral anionic complexes of C_1 symmetry. The potassium K^+ and gadolinium Gd^{3+} ions, occupy the equivalent crystallographic positions of C_2 symmetry. Due to the

distinct difference in the size of K^+ and Gd^{3+} ionic radii, of 1.33 and 1.11, respectively, they occupy the sites in an ordered manner. The structure of KGW is formed by chains of $W_2O_8^{4-}$ ions arranged along the *c*–axis and joined to one another by oxygen atoms with two W–O distances equal to 1.758 Å and 2.359 Å (WOW oxygen bridge bonds). The dimers $W_2O_8^{4-}$ are formed by two WO_4^{2-} ions, which are connected by four W–O bonds of two different lengths equal to 1.955 Å and 2.109 Å (WOOW double oxygen bridge bonds). The lengths of the remaining two W–O bonds are 1.747 Å and 1.825 Å [2]. Along the *b* axis the tungstate – oxygen layers are alternate with the cationic layers made of K^+ and Gd^{3+} ions. In the ytterbium and erbium ions doped KGW crystals the Gd^{3+} ions can be efficiently substituted by Yb^{3+} and Er^{3+} ions [2,12]. For the doping concentration used in this work the crystal structure does not change. The slight change in the cell parameters observed can be a consequence of the different ionic radii of Gd, Er and Yb atoms [4].

The study was undertaken to determine the temperature–dependent vibrational properties of the Er^{3+} doped KGW crystals co-doped with Yb^{3+} ions (KGW : (Er, Yb)) by the Raman scattering method in the 77 – 292 K temperature range. The results obtained are discussed in terms of the influence of temperature on the lattice dynamics and crystal structure.

2. Experimental

KGW : (Er, Yb) single crystals used in the Raman study were obtained using the Top Seeded Solution Growth method from 25 mol % solutions of KGW in $K_2W_2O_7$ on [010] oriented seeds. The detailed description of the technique used can be found

elsewhere [14]. The doping concentration of Er^{3+} and Yb^{3+} ions in the starting melt were 1 at.% and 5 at.%, respectively. The concentrations of the dopants in the as-grown single crystals were not measured. However, according to literature data, the distribution coefficient between the crystal and the melt of lanthanide doped KGW crystals is between 0.88 and 1.02 [3], so the concentration of Er^{3+} and Yb^{3+} ions in as-grown KGW : (Er, Yb) single crystals is close to the concentration in the melt. The crystallographic orientation of the samples was established by the Laue method using the stereographic Wulff net, described in details by Michalski et al. [15]. The oriented samples of the sizes $5 \times 4 \times 3$ mm^3 with faces perpendicular to the [100], [010] and [001] directions were used to collect Raman spectra. The scattered light in the Raman spectrometer used was analyzed by a double grating monochromator and detected by the photon counting system. The argon laser line λ = 488 nm was used for excitation in the Raman experiment. The polarized Raman spectra were recorded in the spectral range 20 – 1000 cm^{-1} with the spectral slit–width of 2 cm^{-1}. The temperature dependent polarized Raman spectra were measured for the *y(xx)z* and *y(xy)z* scattering geometry over the 77 – 292 K temperature range. Taking into regard the Bose–Einstein population factor, the fitting procedure was applied to obtain the band parameters of temperature Raman spectra.

3. Results and discussion

The crystal structure of KGW : (Er, Yb) is isomorphous with the KGW structure. The primitive unit cell of KGW crystals includes two $KGd(WO_4)_2$ units and contains 24 atoms giving 72 fundamental vibrations. From the factor group analysis of

the zone-center modes for the monoclinic structure ($C2/c \equiv C_{2h}^6$) the activity of the 3 acoustic modes $A_u + 2B_u$, 15 translational modes $2A_g + 4B_g + 4A_u + 5B_u$, 6 librational modes $3A_g + 3B_g$ and 48 internal modes $12A_g + 12B_g + 12A_u + 12B_u$ is predicted. Among them $17A_g + 19B_g$ are Raman-active modes [16]. The detail assignment of the modes for $KGd(WO_4)_2$ crystals was proposed by Macalik et al. [12].

From the spectroscopic point of view, the WO_4^{2-} ions are the most important molecular groups in the crystals investigated, as their activity is revealed in the majority of bands in the Raman spectra. The free WO_4^{2-} tetrahedron has the T_d symmetry, giving 15 vibrational degrees of freedom, which can be divided into four internal $\nu_1(A_1)$, $\nu_2(E)$, $\nu_3(F_2)$ and $\nu_4(F_2)$ and two external: rotational – $\nu_R(F_1)$ and translational – $\nu_T(F_2)$ modes. It was found that the vibrational modes of WO_4^{2-} anion in aqueous solutions are located at 931 cm^{-1} ($\nu_1(A_1)$), 320 cm^{-1} ($\nu_2(E)$), 833 cm^{-1} ($\nu_3(F_2)$) and 380 cm^{-1} ($\nu_4(F_2)$) [17]. For tungstate crystals, in which WO_4^{2-} ions form isolated tetrahedra, the internal stretching vibrations $\nu_1(A_1)$ and $\nu_3(F_2)$ occur in the 750 – 1000 cm^{-1} range, while the internal bending vibrations $\nu_2(E)$ and $\nu_4(F_2)$ in the 250 – 430 cm^{-1} range [18]. The primitive unit cell of $KGd(WO_4)_2$ contains four WO_4^{2-} tetrahedra, at equivalent sites in the crystal lattice and in similar surroundings. The symmetry lower than tetragonal one and similar site groups symmetry at these sites produce shifts and splittings of the free WO_4^{2-} tetrahedron vibrational frequencies. The site symmetry of WO_4^{2-} ions is reduced from T_d to C_1 symmetry, because of the influence of the crystal field in the primitive unit cell. Moreover, the coupling between the vibrations of different molecular groups in the crystal lattice leads to further shifts and splittings of the vibrational frequencies of the whole crystal and further changes in the structure of vibrational modes. It was found for

other tungstates that the Ln^{3+} cations surrounding the WO_4^{2-} anions affect the internal vibrations of these anions [18]. Moreover, the Raman spectra of KGW crystals are more complicated due to the existence of the double oxygen bridge bonds WOOW in the crystals. For double bridge bonds WOOW there are six internal vibrational modes for the complex consisting of four atoms. Four of these modes are stretching and two are bending vibrations [13].

To detect A_g and B_g modes of KGW : (Er, Yb) crystals, the Raman spectra were collected in the $y(xx)z$ and $y(xy)z$ scattering geometries, respectively. The polarized Raman spectra of KGW : (Er, Yb) crystals obtained in the 20 – 1000 cm^{-1} spectral range at room temperature are presented in Fig. 1.

Fig. 1

The obtained Raman spectra of KGW : (Er, Yb) crystals cover the range of external and internal vibrational motions. The detailed analysis of polarized Raman spectra allows us to assign the Raman bands as A_g or B_g modes, however, as seen from Fig. 1, most of them are not fully polarized, being active both in the $y(xx)z$ and $y(xy)z$ spectra. The internal vibrational modes of WO_4^{2-} tetrahedra appear in the Raman spectra in the range 270 –1000 cm^{-1}. As follows from Fig. 1, the very intense, sharp peak attributed to $\nu_1(A_1)$ symmetric stretching vibrations of the WO_4^{2-} tetrahedron appears at 899 cm^{-1} as an A_g mode. The $\nu_3(F_2)$ stretching vibrations of the WO_4^{2-} group appear in the spectral range of 740 – 810 cm^{-1}. The strongly polarized A_g band positioned at 744 cm^{-1} is attributed to the coupling stretching vibration of WO_4^{2-} and WOOW, while the A_g band

at 766 cm^{-1} to the stretching vibration of WOOW. The B_g modes detected at 756 and 805 cm^{-1} are attributed to stretching vibrations of WOOW and WOW bridge bonds, respectively. In the spectral range of 400 – 700 cm^{-1}, the stretching and bending vibrations of WOOW and WOW are observed. Depolarized bands at 529 and 685 cm^{-1}, being active with almost the same intensity in the $y(xx)z$ and $y(xy)z$ geometry, are assigned to the in-plane stretching vibrations of the WOOW oxygen bridge bonds. The deformation bending vibrations $\nu_2(E)$ and $\nu_4(F_2)$ of the WO_4^{2-} tetrahedra appear in the spectral range of 270 – 380 cm^{-1}. The bending vibrations of WO_4^{2-} are recorded at 348, 372 cm^{-1} as B_g modes, and the mode observed at 342 cm^{-1} is recorded as an A_g mode. The peaks at 314 and 401 cm^{-1} are attributed to the out-of-plane and in-plane bending of WOW, respectively. Moreover, the bands connected with the bending vibrations of the oxygen WOOW bridge bonds appear at 272, 278 and 298 cm^{-1}. Below 260 cm^{-1}, the lattice modes (librations of WO_4^{2-} ions and translations of WO_4^{2-}, K^+, Gd^{3+} and W^{6+} ions, in-plane and out-of-plane bending of WOOW and WOW bridge bonds, wagging vibrations of the whole W_4O_{20} complex) are observed in the Raman spectra. The dominant band in this spectral range is attributed to the strong translational mode of WO_4^{2-} ions located at 89 cm^{-1}. Most of the bands in this spectral range are active with higher intensity in the $y(xx)z$ geometry, except for the modes at 80, 103, 191 and 252 cm^{-1}, which are fully polarized and observed in the $y(xy)z$ geometry. The detailed assignment all of the modes is presented in Table 1.

Table 1

To determine the influence of temperature on the Ramana spectra, the crystals were investigated on cooling process from 293 K down to 77 K. The spectral analysis of the bands shows minor frequency changes but significant intensity changes in the majority of them. We observed the higher intensity and stronger depolarization of some of them at 77 K than at room temperature. To describe these phenomena we determined the degree of depolarization D as the intensity ratio I_{xy}/I_{xx} and I_{xx}/I_{xy} of the Raman bands detected in the *y(xx)z* and *y(xy)z* scattering geometries for A_g and B_g modes, respectively [19]. The calculated values of D are presented in Table 1, both at 293 and 77 K.

According to Table 1, the depolarization of the majority of Raman bands is higher at 77 K than at room temperature, except for the 527 and 683 cm^{-1} ones, which are strongly depolarized also at room temperature due to the existence of two different crystallographic nonequivalent orientations of the WOOW oxygen bridge bonds in the KGW crystal structure. The observed depolarization of the bands of KGW : (Er, Yb) crystals is due to the distortion of WO_4^{2-} ions from tetrahedral symmetry and the imperfect orientation of molecular groups with respect to the crystallographic axes. Moreover, it can be also caused by the optical activity of KGW : (Er, Yb) crystals leading to rotation of the polarization plane of the incident light, which was earlier observed by us [20]. On cooling the deviation of their orientations grows and the WO_4^{2-} tetrahedra become strongly distorted, which is visible as increased depolarization of particular bands. The WOOW double bridge bonds have two orientations in the crystal structure, which are less sensitive to temperature changes. So, the bands at 527 and 683 cm^{-1} do not change their polarization on cooling from 293 to 77 K.

Temperature dependencies of selected modes of KGW : (Er, Yb) are presented in Figs 2 – 7.

Figs 2(a) and (b)

As follows it is seen from Figs 2(a) and (b), the position of the dominant band of KGW : (Er, Yb) at 899 cm^{-1} does not change the position and the FWHM of this band decreases linearly from 293 to 77 K. The integral intensity of this mode is practically constant in the temperature range 293 – 175 K and then it linearly increases to 77 K. The observed rapid increase in the activity of the symmetric stretching vibration within the WO_4^{2-} ions below 175 K and the increase in the depolarization of the 899 cm^{-1} band at 77 K probably result from the distortion of WO_4^{2-} tetrahedra in the low-temperature region. The frequency of the band at 805 cm^{-1} is almost constant and the FWHM decreases linearly in the temperature range studied.

The strongest temperature changes in the Raman spectra of KGW:(Er, Yb) crystals were observed in the 650 – 850 cm^{-1} spectral range (Fig. 3).

Fig. 3

In this spectral range we detected the peaks assigned to the internal stretching vibrations of WO_4^{2-} ions and the oxygen bridge bonds WOOW and WOW. As shown in Fig. 3, that 744 and 756 cm^{-1} modes, shift insignificantly towards higher frequencies, while the band at 765 cm^{-1} is evidently shifted to lower frequencies at 77 K. Moreover,

the depolarization of 744 and 765 cm^{-1} is significantly higher at 77 K than at room temperature (see Table 1).

Fig. 4(a) and (b)

As shown in Fig. 4(a), the frequencies of 744 and 756 cm^{-1} bands slightly increases, while the 765 cm^{-1} band frequency decreases by 4 cm^{-1} on cooling from 292 down to 77 K. As a results, the peaks at 744 and 765 cm^{-1} separated by 21 cm^{-1} at room temperature are separated by 14 cm^{-1} at 77 K. This anomalous shift of the frequency of the 765 cm^{-1} band with lowering temperature is due to the elongation of W–O bonds in the WOOW bridge bonds, which probably results from strengthening of intermolecular interactions between the adjacent WO_4^{2-} ions. Moreover, the temperature dependence of FWHM of the bands at 744 and 756 cm^{-1} changes linearly with temperature, while the mode at 765 cm^{-1} shows the slightly different slope below and above 175 K (inset of Fig. 4(b)). The nonlinear narrowing of this band indicates some higher disorder above 175 K related to WO_4^{2-} ions, which are freer in the KGW : (Er, Yb) crystals than the strong and more rigid oxygen bridge bonds WOOW. Also, according to Fig. 4b, the integrated intensity of 765 cm^{-1} mode does not change between 293 K and 175 K, however, we observe the linear increase on cooling below 175 K indicating an increase in the activity of this mode.

The temperature dependencies of selected stretching vibrations of the double oxygen bridge bonds WOOW are presented in Figs 5(a) and (b). The mode positioned at 683 cm^{-1} at room temperature shifts by 3 cm^{-1} from 293 to about 175 K and then its position is almost constant down to 77 K. The position of the mode at 527 cm^{-1} is

temperature insensitive. The integrated intensity of the 683 and 527 cm^{-1} modes is comparable in the whole temperature range and changes similarly with temperature (Fig. 5(b)). The FWHM of these modes decreases linearly on cooling to 77 K. The depolarization of these bands does not change with temperature. This probably results from very small changes in the orientations of the WOOW oxygen bridge bonds in the crystal structure. The stable character of changes indicates the presence of a very strong and rigid character of the W–O bonds in WOOW bridge bonds.

Fig. 5(a) and (b)

The bending modes of WO_4^{2-} ions located at 343, 348 and 372 cm^{-1} do not significantly change their position on cooling to 77 K (Fig. 6). However, we observe the small anomaly in frequency at about 175 K, which results from distortion of WO_4^{2-} tetrahedra. On the other hand no anomaly in the temperature dependence of FWHM is observed, which indicates very slight influence of temperature on the bending vibrations of the WO_4^{2-} tetrahedra.

Fig. 6

In the region of the lattice modes we observed a significant increase in the intensity of most of the bands. In Fig. 7(a) and (b) present the temperature dependencies of the frequency and integrated intensity of two selected lattice modes positioned at 89 and 206 cm^{-1} are presented.

Fig. 7(a) and (b)

The mode centered at 206 cm^{-1} shows a slight shift to a higher frequencies with decreasing temperature, while the frequency of the mode at 89 cm^{-1} insignificantly decreases by about 2 cm^{-1} on cooling. This strong lattice mode practically does not change its position and FWHM. However, its integral intensity shows a significant increase, with an anomaly at about 175 K. Probably at this temperature the slightly disturbed translational motion of the whole tungstate – oxygen layers appears.

4. Conclusions

The results obtained have revealed the depolarization of the majority of the Raman bands in the spectra of KGW : (Er, Yb) crystals at room temperature. The depolarization some of stretching and bending modes is due to the distortion of WO_4^{2-} ions from the tetrahedral symmetry and their imperfect orientation with respect to the crystallographic axes. On cooling from 293 to 77 K, most of the bands show minor frequency changes. However, the 765 cm^{-1} mode exhibits an anomalous shift towards lower frequency. The anomalous shift of the frequency of this mode with lowering temperature is due to the elongation of the W–O bonds in the WOOW bridge bonds, which results from stronger intermolecular interactions between the adjacent WO_4^{2-} ions. Some anomalous changes in the spectral parameters of modes related to the tungstate-oxygen vibrations in the oxygen tetrahedra WO_4^{2-} and the oxygen bridge bonds WOOW in the temperature range 150 – 175 K have been revealed. The rapid increase in the integral intensity of the 899 cm^{-1} mode below 175K, the nonlinear narrowing and increase in the integral intensity of

the 765 cm^{-1} band with lowering temperature and the small anomaly in frequency of the bending modes at 343, 348 and 372 cm^{-1} observed at about 175K, result from the stronger distortion of the WO_4^{2-} tetrahedra in the low-temperature range. The bands at 529 and 685 cm^{-1} assigned to the stretching vibrations of the WOOW oxygen bridge bonds seem to be less temperature sensitive. The anomalies of spectral parameters observed in the temperature range studied are weak, but clearly indicate the lowering of the local symmetry of the KGW : (Er, Yb) crystal structure.

Acknowledgments

This work was financed by the Research Project: MNiI 1 P03B 058 27.

References

1. A.A. Kaminskii, L. Li, A.V. Butashin, V.S. Mironov, A.A. Pavlyuk, S.N. Bagayev, K. Ueda, New crystalline lasers on the base of monoclinic $KR(WO_4)_2:Ln^{3+}$ tungstates (R=Y and Ln), Opt. Rev. 4 (1997) 309-315.
2. M.C. Pujol, M. Rico, C. Zaldo, R. Solé, V. Nikolov, X. Solans, M. Aquiló, F. Díaz, Crystalline structure and optical spectroscopy of Er^{3+}-doped $KGd(WO_4)_2$ single crystals, Appl. Phys. B 68 (1992) 187-197.
3. C. Pujol, M. Aguiló, F. Díaz, C. Zaldo, Growth and characterization of monoclinic $KGd_{1-x}RE_x(WO_4)_2$ single crystals, Opt. Mater. 13 (1999) 33-40.
4. J. Lancok, C. Garapon, V. Vorliček, M. Jelinek, M. Čerňanskỳ, Structural and fluorescence properties of thin films fabricated by pulsed laser deposition technique from Nd:KGW single crystal, Opt. Mater. 28 (2006) 360-369.
5. X. Mateos, R. Solé, J. Gavalda, M. Aguiló, J. Massons, F. Díaz, Crystal growth, optical and spectroscopic characterization of monoclinic $KY(WO_4)_2$ co-doped with Er^{3+} and Yb^{3+}, Opt. Mater. 28 (2006) 423-431.
6. M. Rico, M.C. Pujol, X. Mateos, J. Massons, C. Zaldo, M. Aguiló, F. Díaz, Yb sensitizing of Er^{3+} up-conversion emission in $KGd(WO_4)_2$:Er:Yb single crystals, J. All. Comp. 323-324 (2001) 362-366.
7. X. Mateos, M.C. Pujol, F. Güell, R. Solé, J. Gavalda, J. Massons, M. Aguiló, F. Díaz, Infrared-to-green up-conversion in Er^{3+}, Yb^{3+}-doped monoclinic $KGd(WO_4)_2$ single crystals, Opt. Mater. 27 (2004) 475-479.
8. T.T. Basiev, A.A. Sobol, Yu.K. Voronko, P.G. Zverev, Spontaneous Raman spectroscopy of tungstate and molybdate crystals for Raman lasers, Opt. Mater. 15 (2000) 205-216.

9. L. Macalik, J. Hanuza, B. Macalik, W. Ryba – Romanowski, S. Gołąb, A. Pietraszko, Optical spectroscopy of Dy^{3+} ions doped in $KY(WO_4)_2$ crystals, J. Luminescence 79 (1998) 9-19.
10. L. Macalik, J. Hanuza, A.A. Kamiński, Polarized Raman spectra of the oriented $NaY(WO_4)_2$ and $KY(WO_4)_2$ single crystals, J. Mol. Struct. 555 (2000) 289-297.
11. M. Mączka, J. Hanuza, S. Kojima, J.H. Van der Maas, Vibrational study of phase transitions in $KIn(WO_4)_2$, J. Sol. State Chem. 158 (2001) 334-342.
12. L. Macalik, J. Hanuza, A.A. Kaminskii, Polarized infrared and Raman spectra of $KGd(WO_4)_2$ and their interpretation based on normal coordinate analysis, J. Raman Spectrosc. 33 (2002) 92-103.
13. M. Mączka, Vibrational characteristics of the alkali metal-indium double molybdates $M\text{In}(MO_4)_2$ and tungstates $M\text{In}(WO_4)_2$ (M=Li, Na, K, Cs), J. Sol. State Chem. 129 (1997) 287-297.
14. A. Majchrowski, M.T. Borowiec, E. Michalski, Top seeded solution growth of $KHo(WO_4)_2$ single crystals, J. Cryst. Growth 264 (2004) 201-207.
15. E. Michalski, A. Majchrowski, Analytical use of the stereographic Wolff net for single-crystal orientation for 1-, 2- and 3-rotated cuts, J. Appl. Cryst. 36 (2003) 255-259.
16. D.L. Rousseau, R.P. Bauman, S.P.S. Porto, Normal mode determination in crystals, J. Ram. Spectrosc. 10 (1981) 253-290.
17. W. Hayes, R. Loudon, Scattering of light by crystals, Dover Publications, Inc., Mineola, New York, 2004.

18. Yu. K. Voronko, A.A. Sobol, S.N. Ushakov, L. Tsymbal, Raman spectra and phase transformations of the $MLn(WO_4)_2$ (M=Na, K; Ln=La, Gd, Y, Yb) tungstates, Inorg. Mat. 36 (9) (2000) 947-953.

19. D. Kasprowicz, T. Runka, M. Szybowicz, P. Ziobrowski, A. Majchrowski, E. Michalski, M. Drozdowski, Characterization of bismuth triborate single crystal using Brillouin and Raman spectroscopy, Cryst. Res. Technol. 40 4/5 (2005) 459-465.

20. D. Kasprowicz, S. Mielcarek, A. Trzaskowska, A. Majchrowski, E. Michalski, M. Drozdowski, Elastic properties of $KGd(WO_4)_2$:Ho^{3+} single crystals studied by Brillouin spectroscopy, Cryst. Res. Technol. 42 (2007) 1370-1375.

Figure Captions

Fig. 1. Raman spectra of KGW : (Er, Yb) crystals for the *y*(*xx*)*z* and *y(xy)z* scattering geometries.

Fig. 2. Temperature dependencies of the stretching vibrational modes of KGW : (Er, Yb) crystal (a) frequency of 805 and 899 cm^{-1} modes, (b) integral intensity and FWHM of 899 cm^{-1} mode.

Fig. 3. Raman spectra of KGW : (Er, Yb) crystals for the *y*(*xx*)*z* and *y*(*xy*)*z* scattering geometry in the 650 cm^{-1} – 850 cm^{-1} spectral range at 293 and 77 K. The marked position of Raman bands are determined at room temperature.

Fig. 4. Temperature dependencies of the stretching vibrational modes of KGW : (Er, Yb) crystals (a) frequency of 744, 756 and 765 cm^{-1} mode, (b) integral intensity and FWHM of 765 cm^{-1} mode.

Fig. 5. Temperature dependencies of the stretching vibrational modes of the double oxygen bridge bonds WOOW of KGW : (Er, Yb) crystals (a) frequency of 527 and 683 cm^{-1} modes, (b) integral intensity 527 and 683 cm^{-1} modes.

Fig. 6. Temperature dependencies of the bending vibrational modes of the WO_4^{2-} tetrahedra of KGW : (Er, Yb) crystals in the spectral range 340 – 375 cm^{-1}.

Fig. 7. Temperature dependences of the lattice modes of KGW : (Er, Yb) crystals (a) frequency of 89 and 206 cm^{-1} mode, (b) integral intensity and FWHM of 89 cm^{-1} mode.

Table 1. The wavenumber values [cm^{-1}], degree of depolarization D and assignment of Raman-active modes of KGW : (Er ,Yb) crystals at 293 and 77 K.

Mode	*y(xx)z*	*y(xy)z* 293 K	D	*y(xx)z*	*y(xy)z* 77 K	D	Assignment
B_g		928 vw			928 w		$\nu(WO_4^{2-})+\nu(WOW)$
A_g	899 vs	899 m	0.33	899 vs	900 s	0.70	$\nu(WO_4^{2-})$
B_g	805 w	805 s	0.12	806 m	806 s	0.32	$\nu(WOW)+\nu(WO_4^{2-})$
A_g	765 vs	766 m	0.41	761 vs	761 vs	0.69	$\nu(WOOW)$
B_g		756 sh			757 sh		$\nu(WOOW)+\nu(WO_4^{2-})$
A_g	744 m	744 sh	0.21	747 s	747 m	0.49	
B_g	685 w	683 w	0.59	687 m	687 m	0.62	$\nu(WOOW)$
B_g	529 w	527 w	0.64	529 m	527 m	0.63	
A_g	436 m	436 w	0.43	437 s	437 m	0.72	$\delta(WOW)$
B_g		410 vw			410 w		
A_g	401 vw	401vw	0.56	402 w	402 w	0.93	$\nu(WOW)$
B_g	371vw	372 m	0.09	373 w	374 s	0.18	$\delta(WO_4^{2-})$
B_g	348 w	348 m	0.11	348 m	348 s	0.29	
A_g	342 m	343 w	0.41	342 m	341 m	0.59	
A_g	314 w	314 vw	0.76	313 m	313 m	0.99	$\gamma(WOW)$
B_g	297 vw	298 w	0.13	299 w	299 m	0.25	$\delta(WOOW)+\delta(WO_4^{2-})$
B_g		278 vw		280 vw	281 vw	0.24	
A_g	272 vw			273 vw			
B_g		252 vw			255 vw		$T'(K^+)$
A_g	235 m	236 w	0.40	236 m	236 m	0.77	
A_g	206 m	206 w	0.55	208 m	208 m	0.95	$T'(Gd^{3+})$
B_g		192 w			191 w		
A_g	175 m	175 w	0.42	178 m	178 m	0.76	$\gamma(WOOW)+T'(K^+)$
A_g	150 w	150 vw	0.12	151 w	151 w	0.96	
B_g		142 vw			140 vw		
B_g		131 vw					
A_g	123 w	123 vw	0.58	122 w	122 vw	0.37	
A_g	115 m	115 vw	0.25	113 m	113 w	0.30	$L(WO_6)+\gamma(WOW)$
B_g		103 vw			102 vw		$\gamma(WOOW)+T'(W^{6+},Gd^{3+})$

A_g	89 vs	88 m	0.18	87 vs	88 m	0.24	$T'(W^{6+})$
B_g		80 w			80 w		

abbreviations: vw – very weak; w – weak; m – medium; s – strong; vs – very strong; sh – shoulder; ν - stretching in-plane modes; δ - bending in-plane modes; γ - out-of-plane bending modes; T' - translatory modes; L - libratory modes.

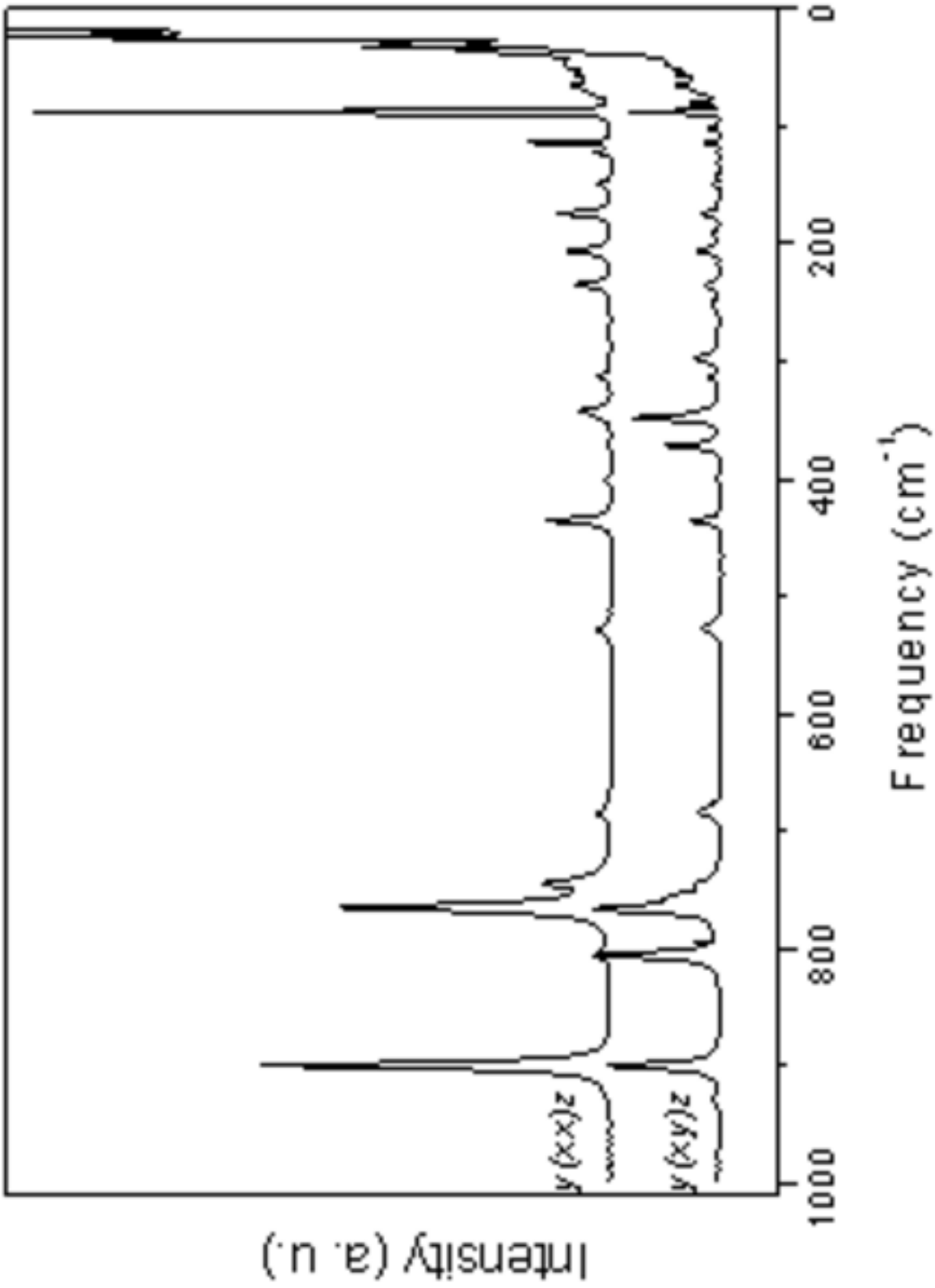

figure1

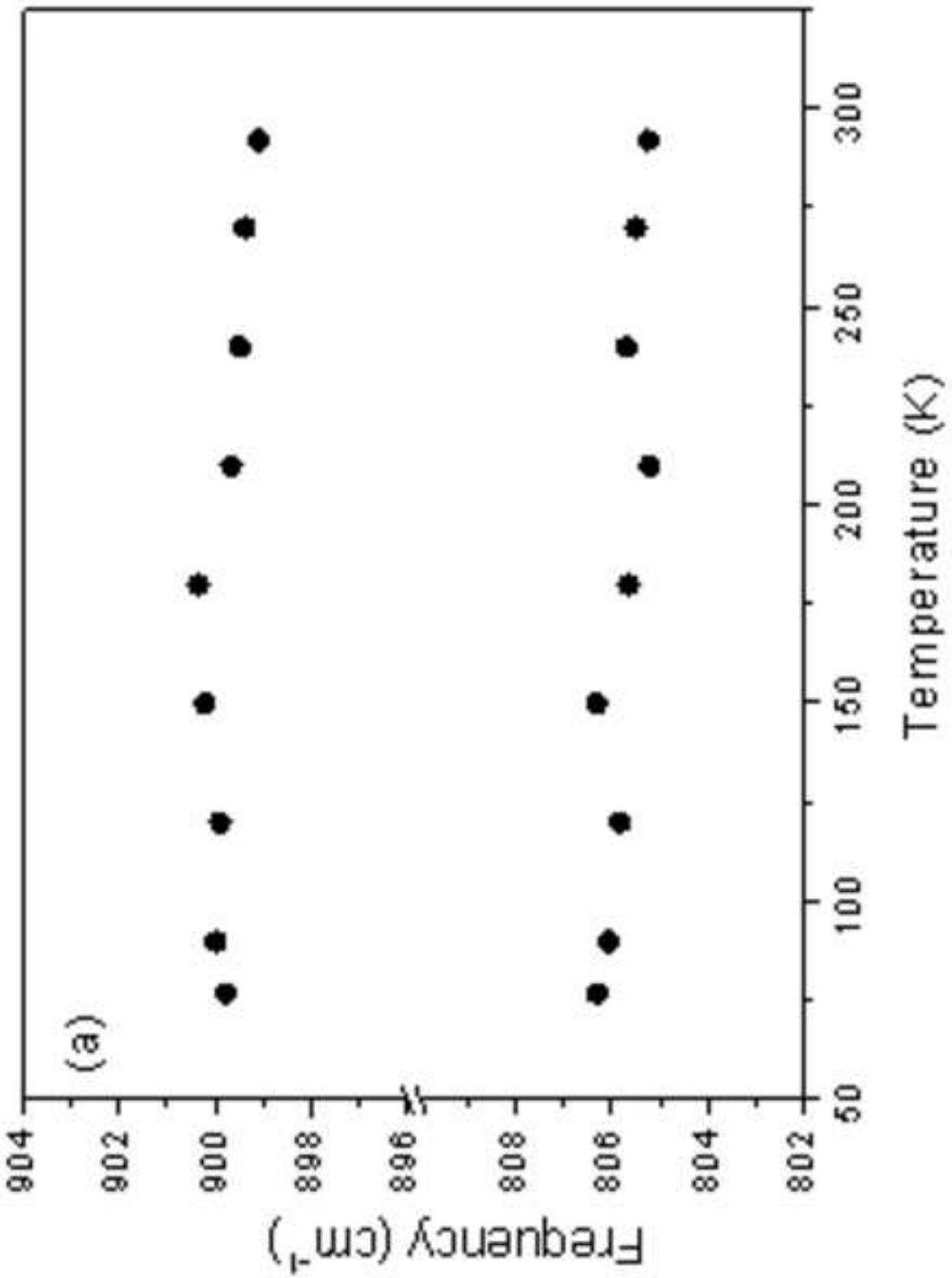

figure2a

figure2b

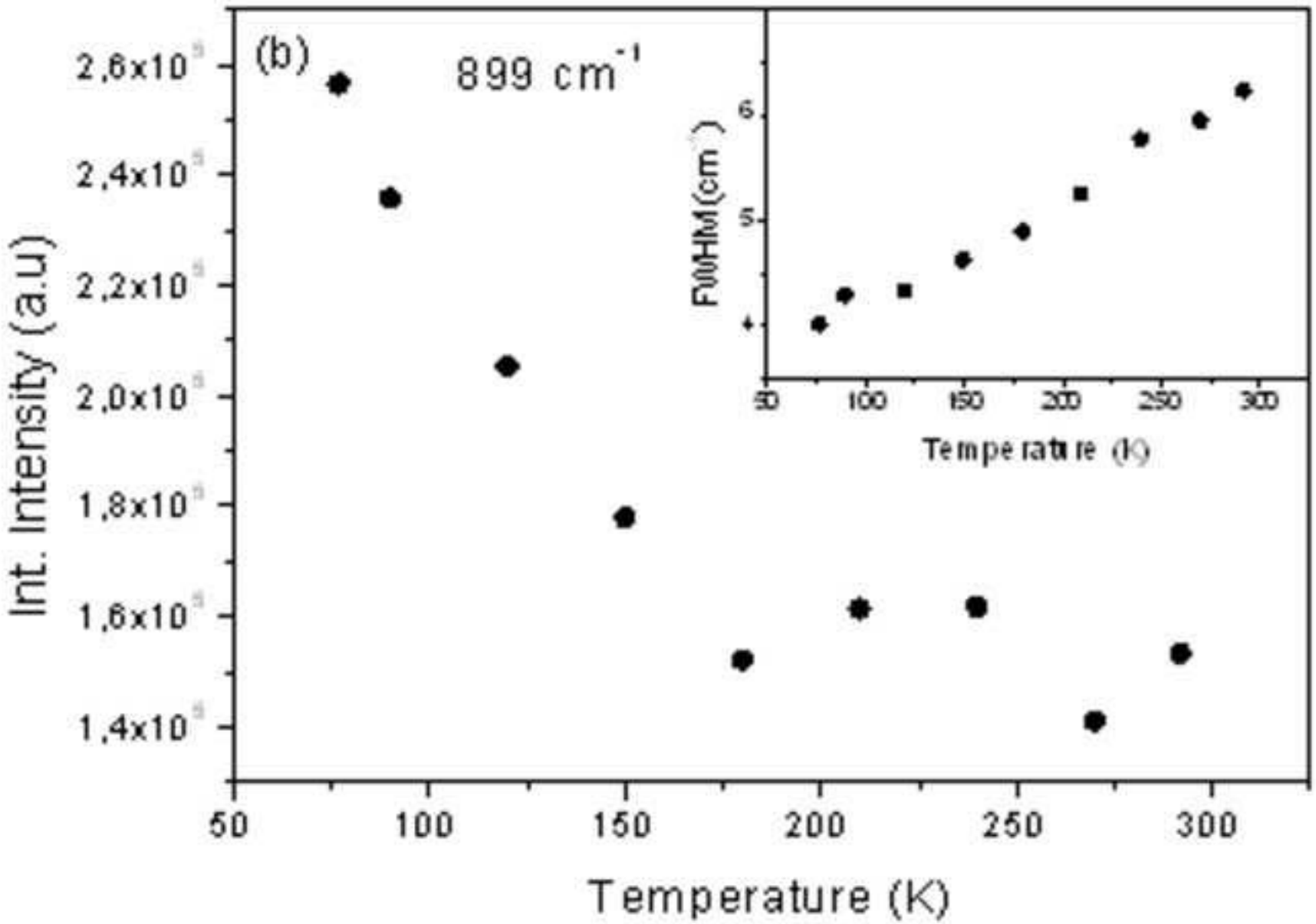

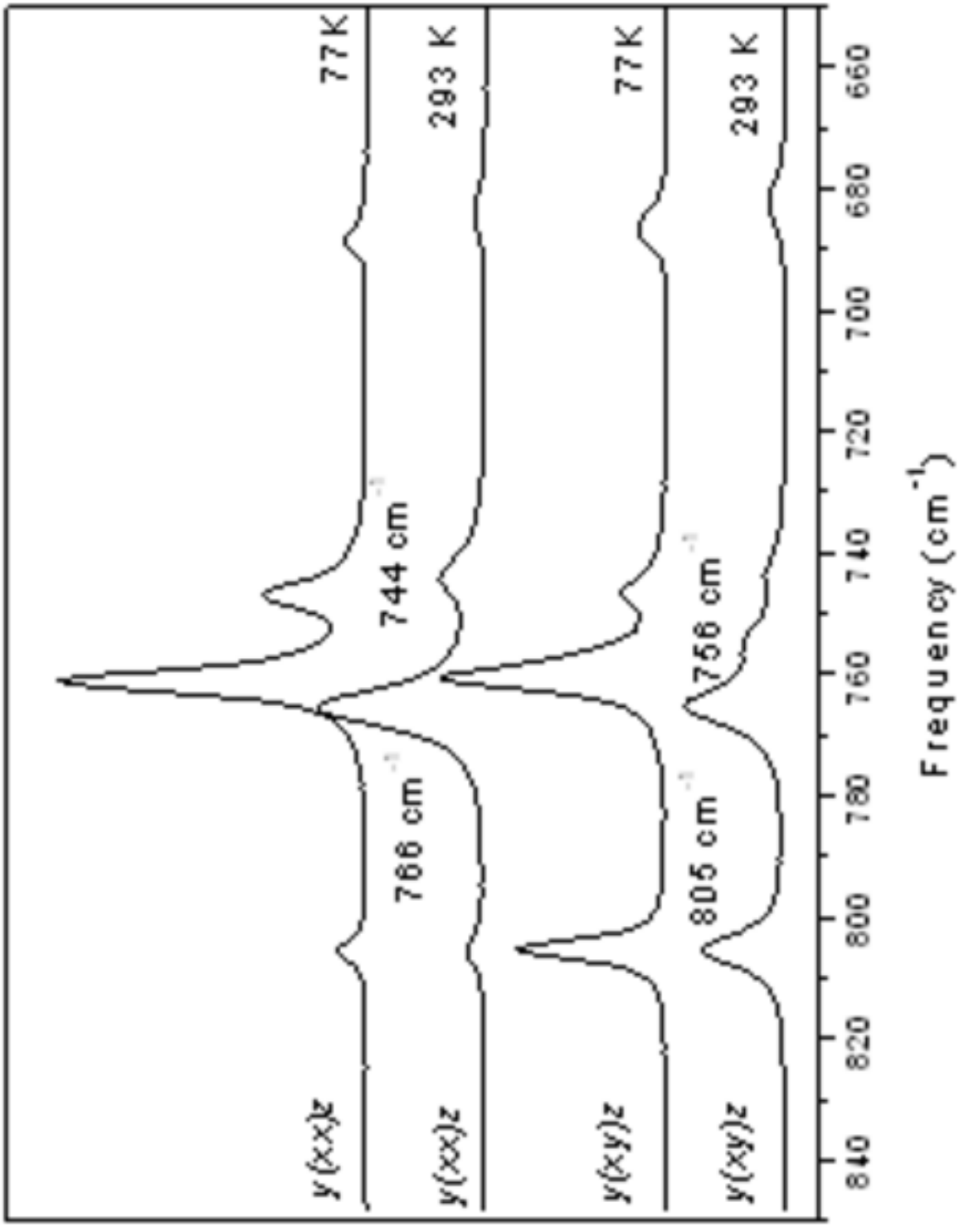

figure3

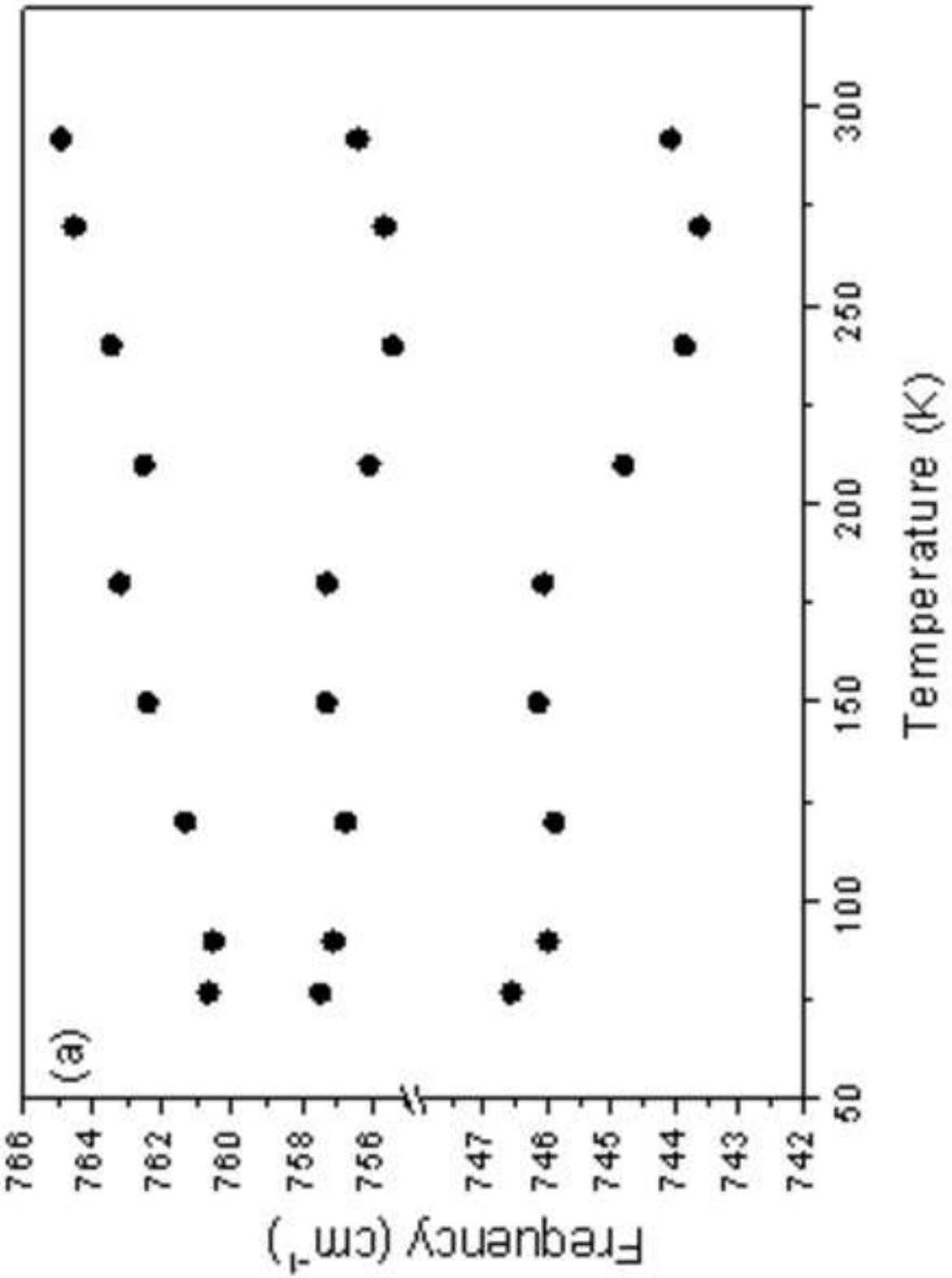

figure4a

figure4b

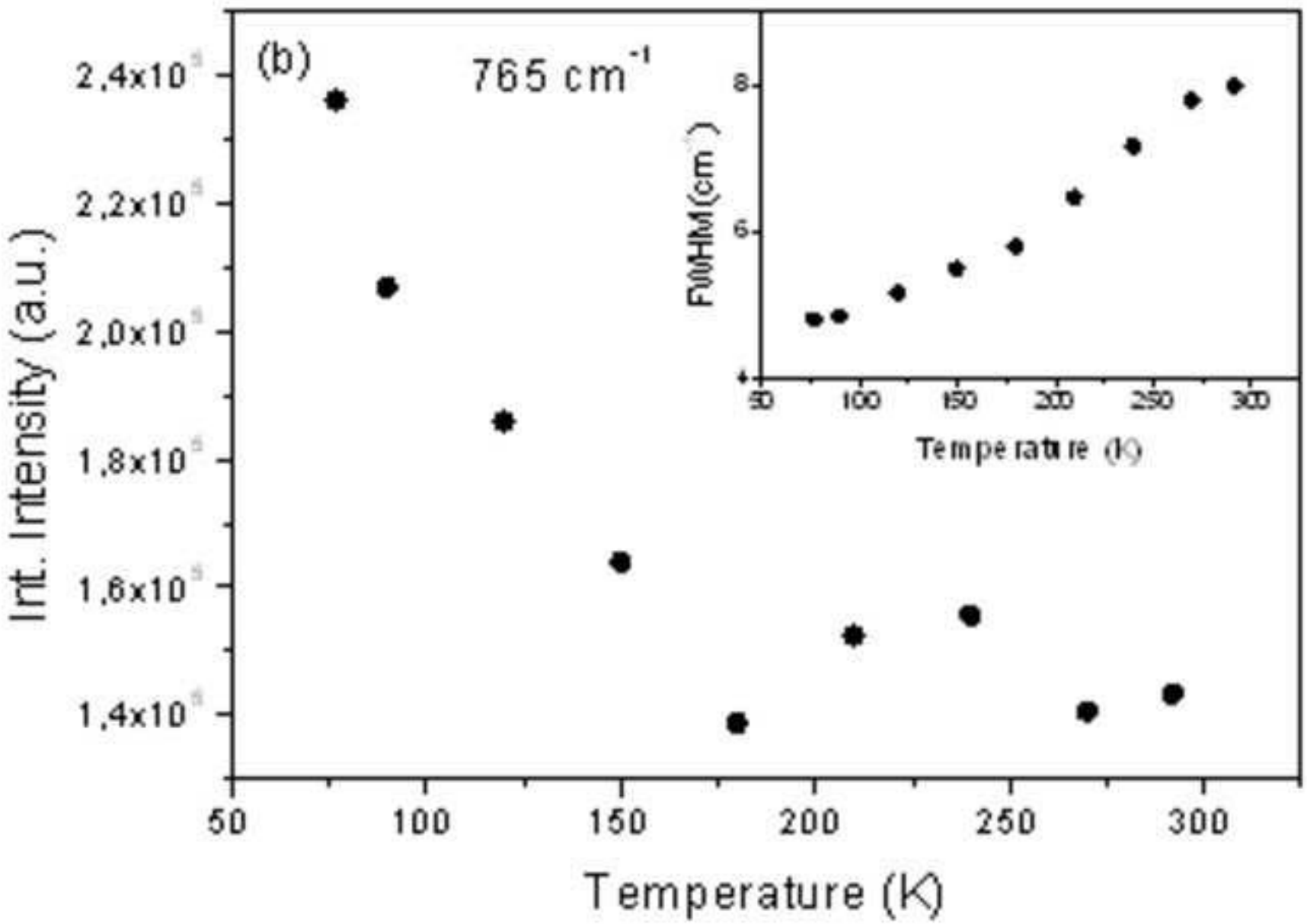

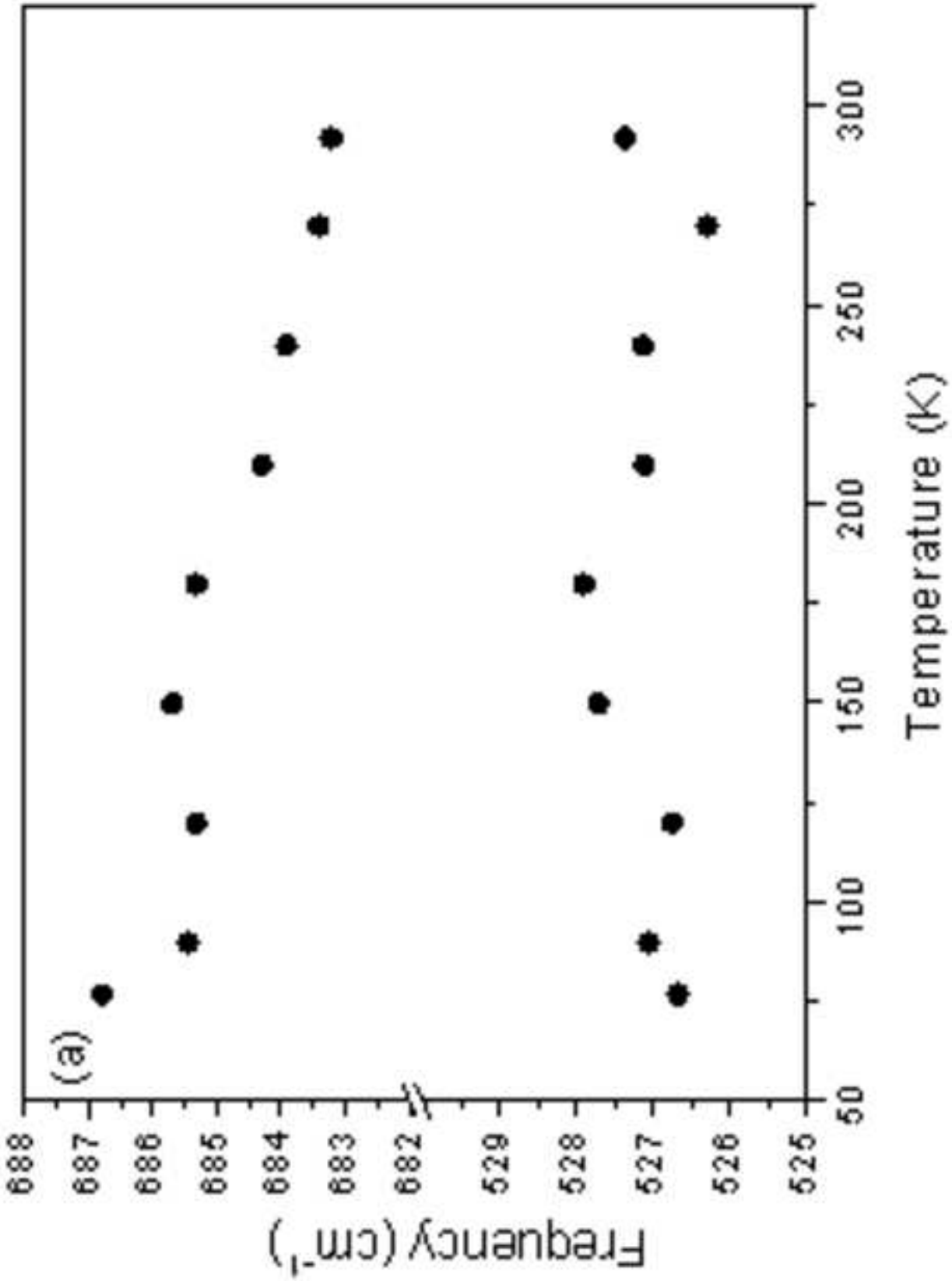

figure5a

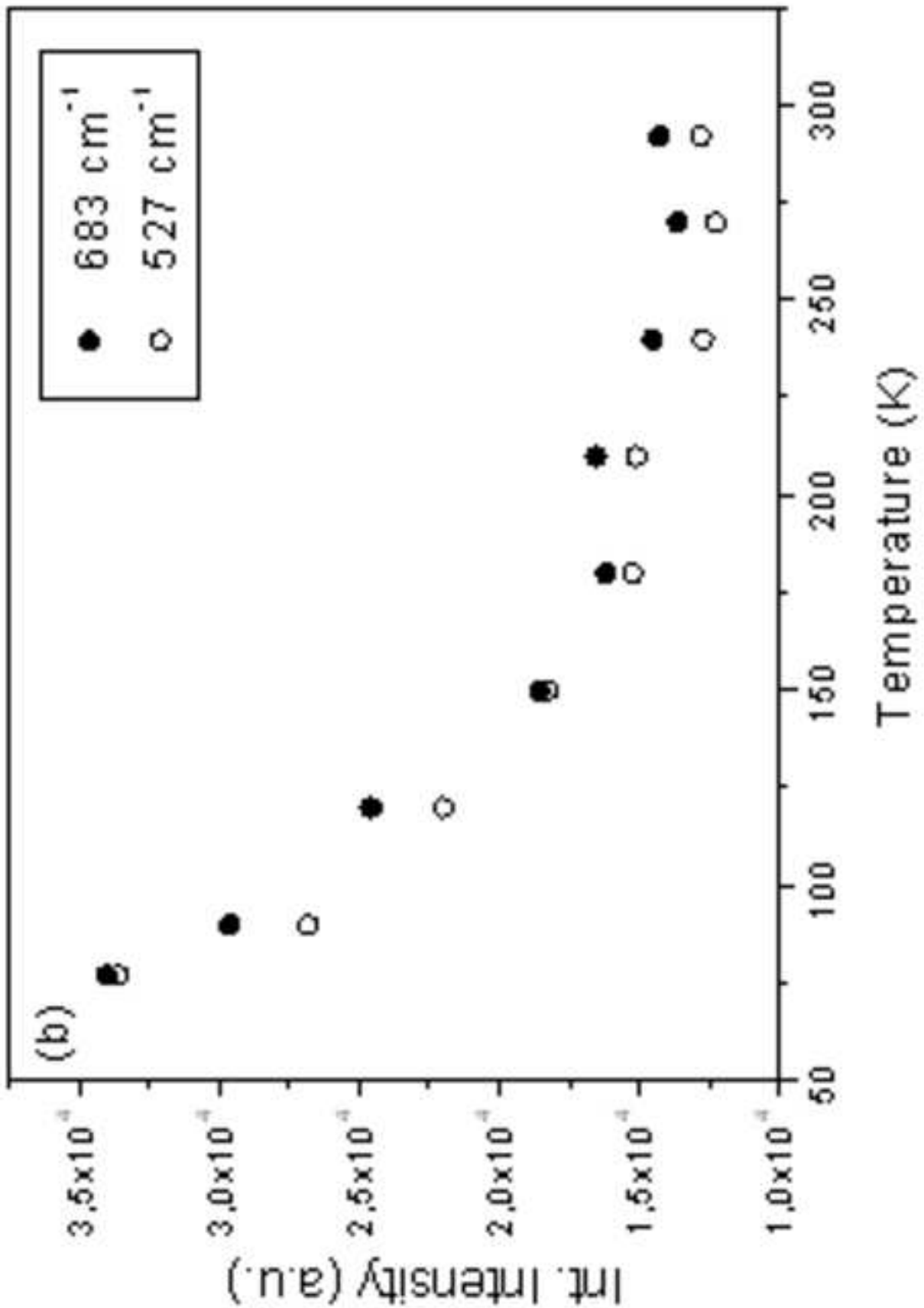

figure5b

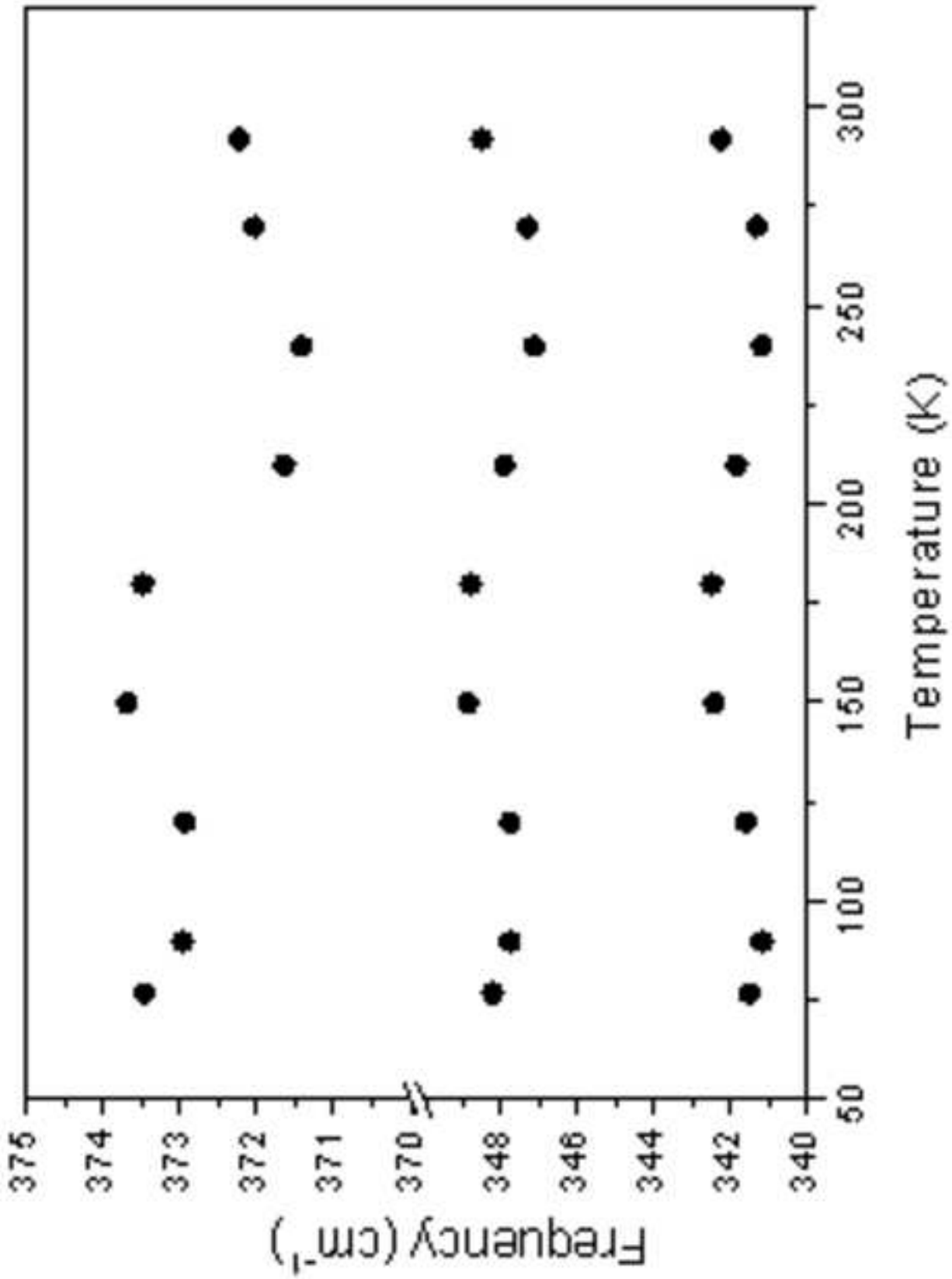

figure6

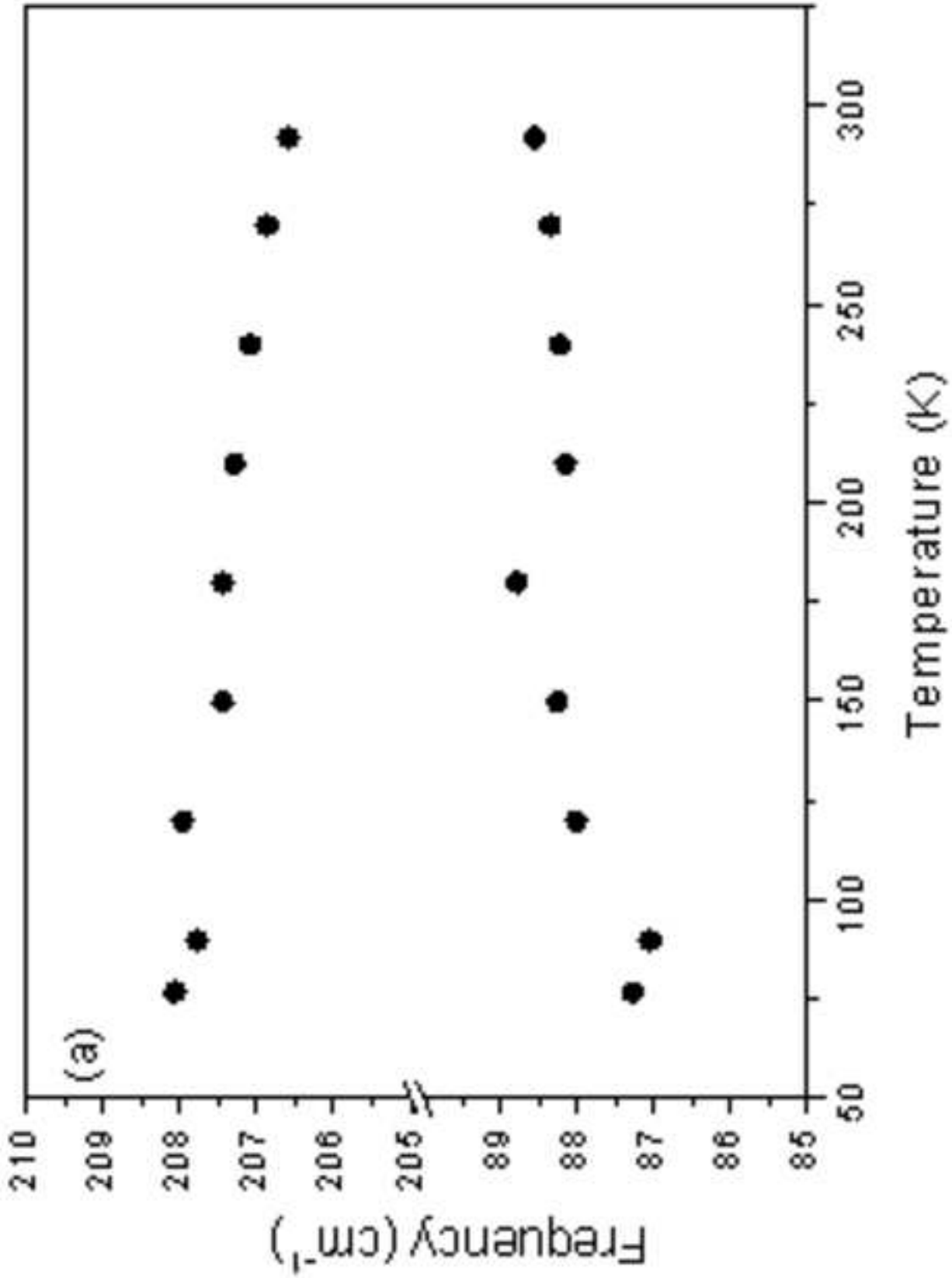

figure7a

figure7b